

Supporting Information

Demystifying the molecular basis of pyrazoloquinolinones recognition at the Extracellular $\alpha 1 + / \beta 3$ - Interface of the GABA_A Receptor by molecular modeling

Natesh Singh,^{1,2,*} Bruno O. Villoutreix¹

¹Univ. Lille, INSERM, Institut Pasteur de Lille, U1177 - Drugs and Molecules for living Systems, F-59000, Lille, France

²University of Vienna, Department of Pharmaceutical Chemistry, Althanstrasse 14, 1090 Vienna, Austria

Contents

Figure S1	2
Figure S2	3
Figure S3	4
Figure S4	5
Figure S5	6
Figure S6	7
Figure S7	8
Table S1.....	9
Figure S8	9
Figure S9	10
Figure S10	10
Figure S11	11
Figure S12	12
Figure S13	13
Figure S14	13
Figure S15	14
Figure S16	15

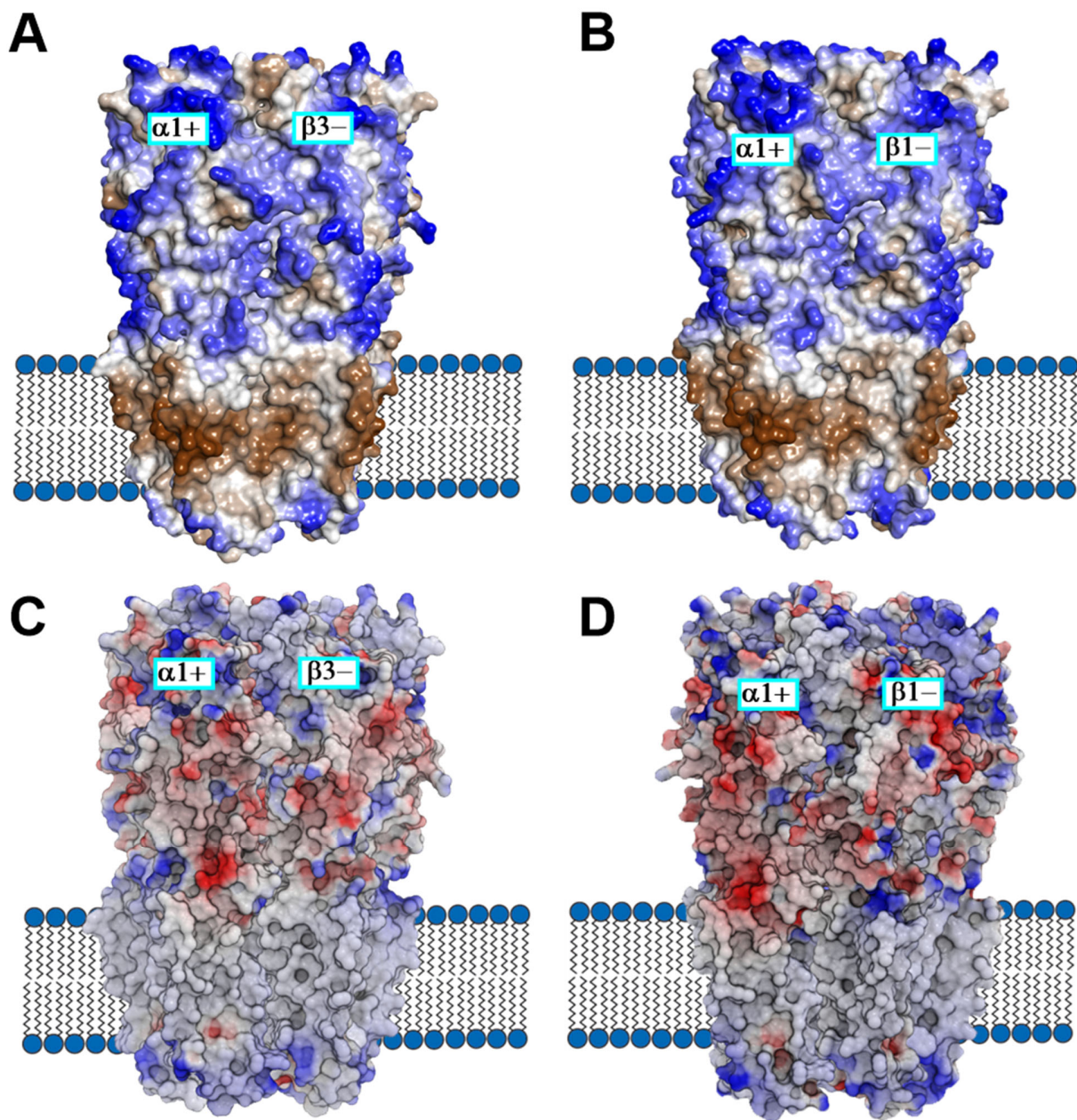


Figure S1. The hydrophobic-hydrophilic surface of the human $\alpha 1\beta 3\gamma 2$ (A) and $\alpha 1\beta 1\gamma 2$ (B) subtypes of the GABA_A receptor. The blue regions correspond to the hydrophilic residues, while the brown areas correspond to the hydrophobic residues. (C) and (D) show the molecular surface colored by the electrostatic potential of the two models, respectively. The electrostatic potential values on the surface range from negative -5 kbT/ec (red) to 5 kbT/ec (blue).

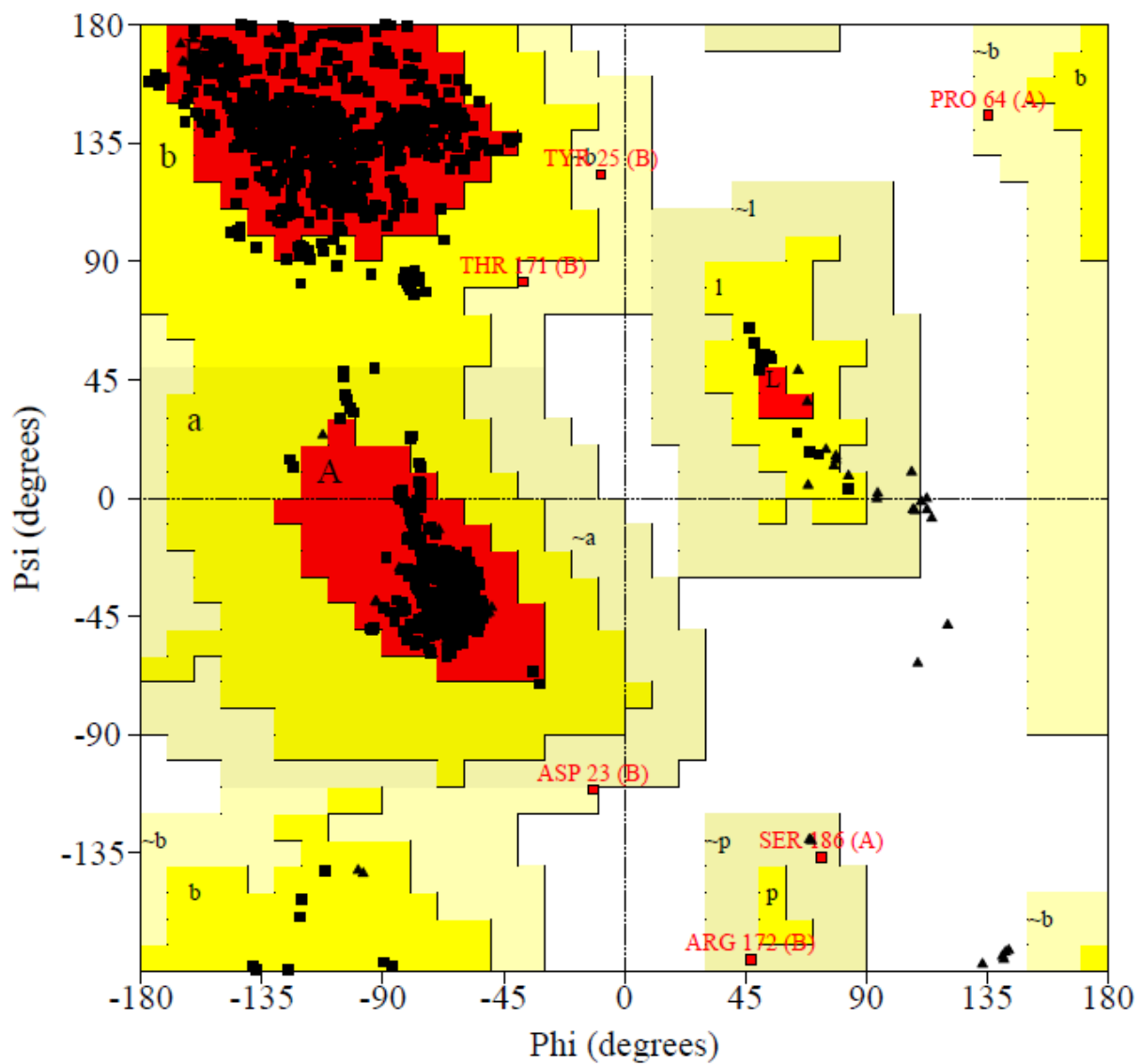


Figure S2. The Ramachandran plot of the $\alpha 1\beta 3\gamma 2$ subtype of the GABA_A receptor based on the 4COF structure.

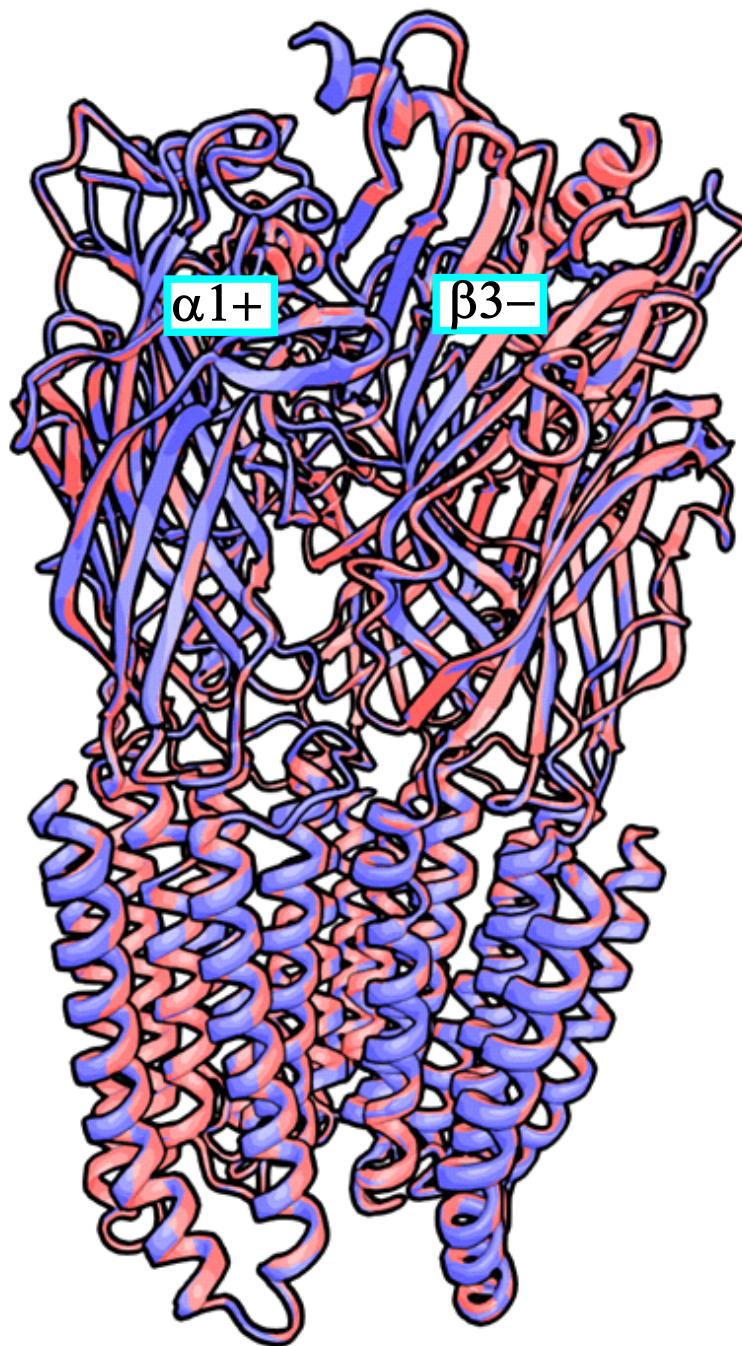


Figure S3. Superimposition of the $\alpha 1\beta 3\gamma 2$ subtype of the GABA_A receptor (red) and the template X-ray structure (2.97 Å) of the human GABA_A $\beta 3$ homopentamer (PDB ID: 4COF) (blue). Backbone RMSD: 0.328 Å, Alignment Score: 0.008.

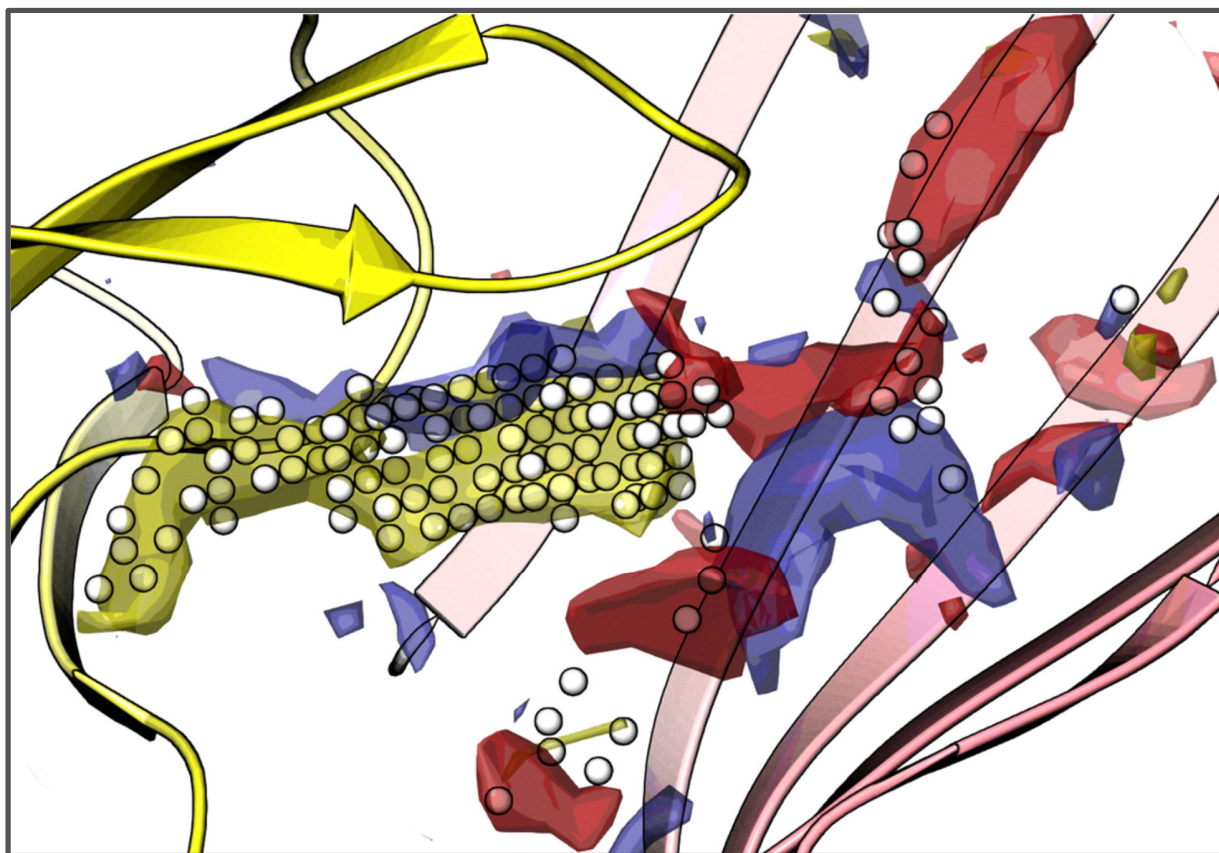


Figure S4. Binding site map of the $\alpha 1+/\beta 3-$ site. (Yellow: Hydrophobic area, Blue: Hydrogen bond donor, Red: Hydrogen bond acceptor, White spheres: Site points).

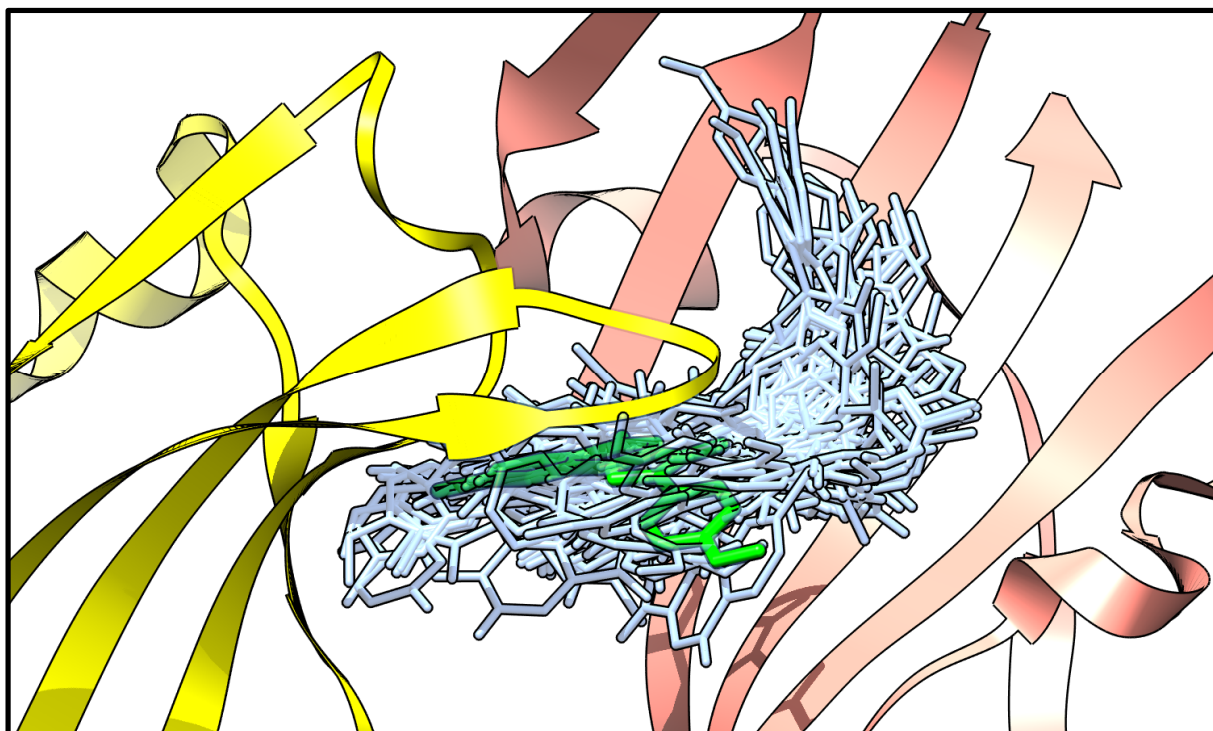


Figure S5. Distribution of the 100 docking poses of PZ-II-028 (**14**) at the $\alpha1+/\beta3-$. A considerable number of poses is observed, some are moderately outside the main pocket, while the rest of the poses are positioned within the pocket. Pose 53 (BM I) is indicated in green and is rendered more prominent, while the rest of the poses are depicted in blue and are made less noticeable. The $\alpha1+$ and $\beta3-$ subunits are shown in ribbon style and are colored yellow and red, respectively.

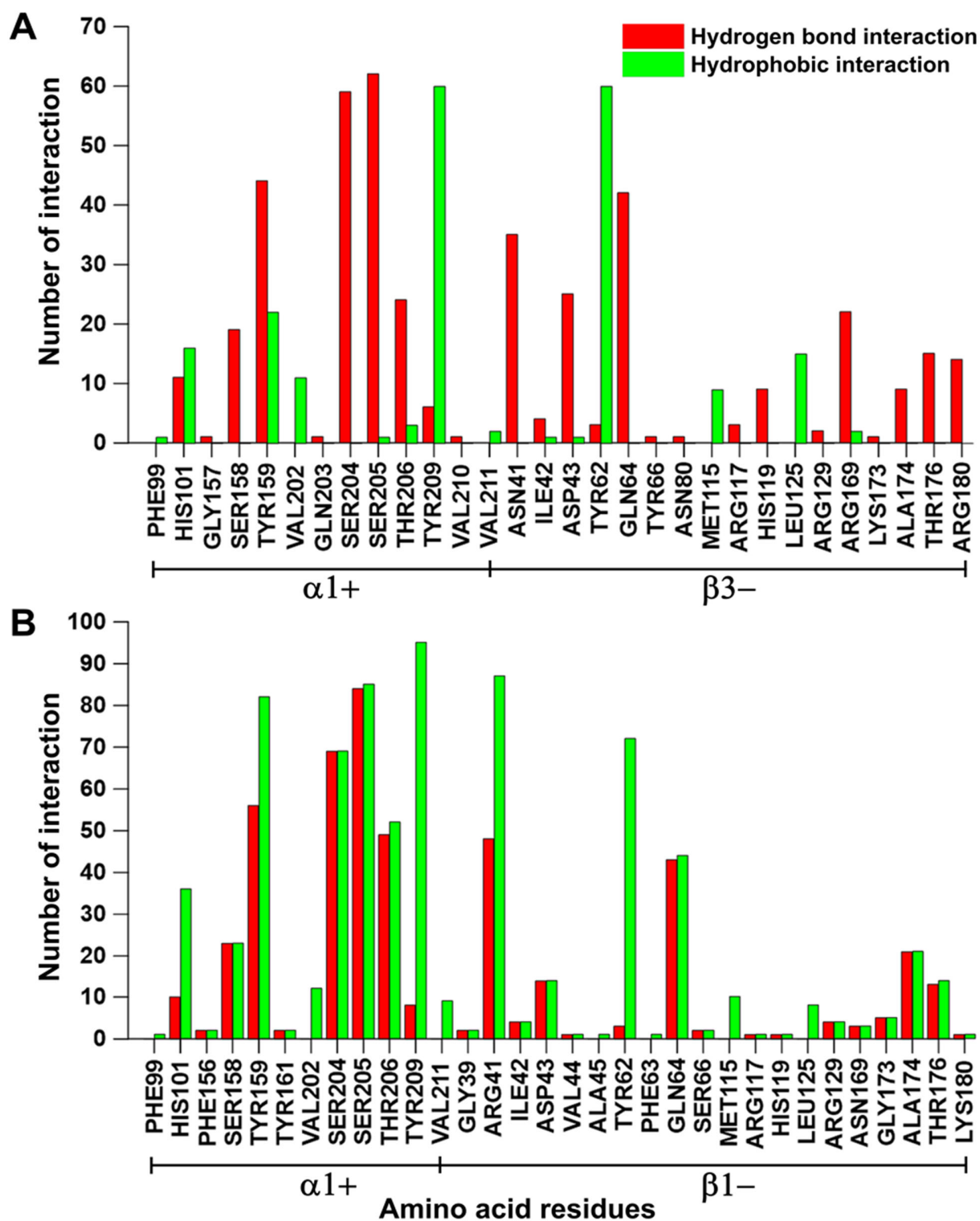


Figure S6. SIFt showing the favorable contacts (hydrogen bond + hydrophobic interactions) of the 100 docking poses of compound **14** at the $\alpha 1+/\beta 3-$ (A) and $\alpha 1+/\beta 1-$ interface (B). $\alpha 1Y159$,

$\alpha 1S204$, $\alpha 1S205$, $\alpha 1T206$, $\beta 1R41$, and $\beta 1Q64$, were the key residues involved in hydrogen bond interactions with the docking poses at the $\alpha 1+/\beta 1-$, while the residues $\alpha 1Y159$, $\alpha 1S204$, $\alpha 1S205$, and $\alpha 1Y209$, $\beta 1R41$, and $\beta 1Y62$ contributed to the binding through hydrophobic interactions. Overall, the SIFt analysis indicated major hydrophobic interactions in the docking poses at the $\alpha 1+/\beta 1-$ as compared to the poses at the $\alpha 1+/\beta 3-$ that seems consistent with the low affinity of **14** at the $\alpha 1+/\beta 3-$ as compared to the $\alpha 1+/\beta 1-$.

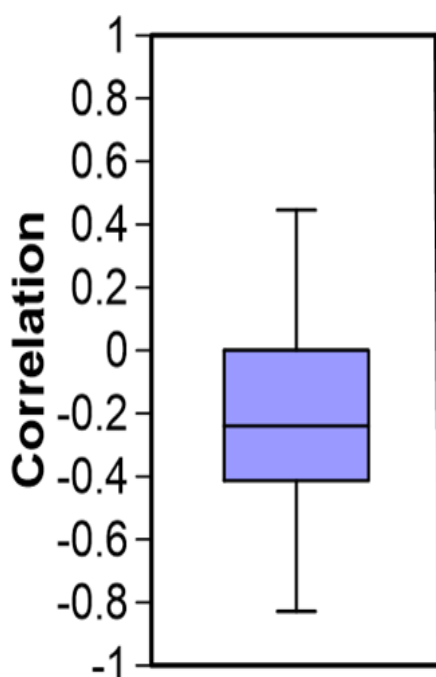


Figure S7. Distributions of Pearson correlation values obtained by quantitative assessment of the 100 docking poses of PQs, at the $\alpha 1+/\beta 3-$, between measured and predicted binding affinity values. In the box plots, the central horizontal line represents the median value, whereas the lower and upper horizontal lines are the first and third quartiles of the distribution. The whiskers go from each quartile to the minimum or maximum.

pose	p56	P60	p66
p53	3.25	2.95	2.87
p56	-	4.07	4.13
p60	-	-	2.23

Table S1. The RMSD (Å) between the top-ranked ranked poses in $\alpha 1\beta 3$ identified from the SAR congruency calculations.

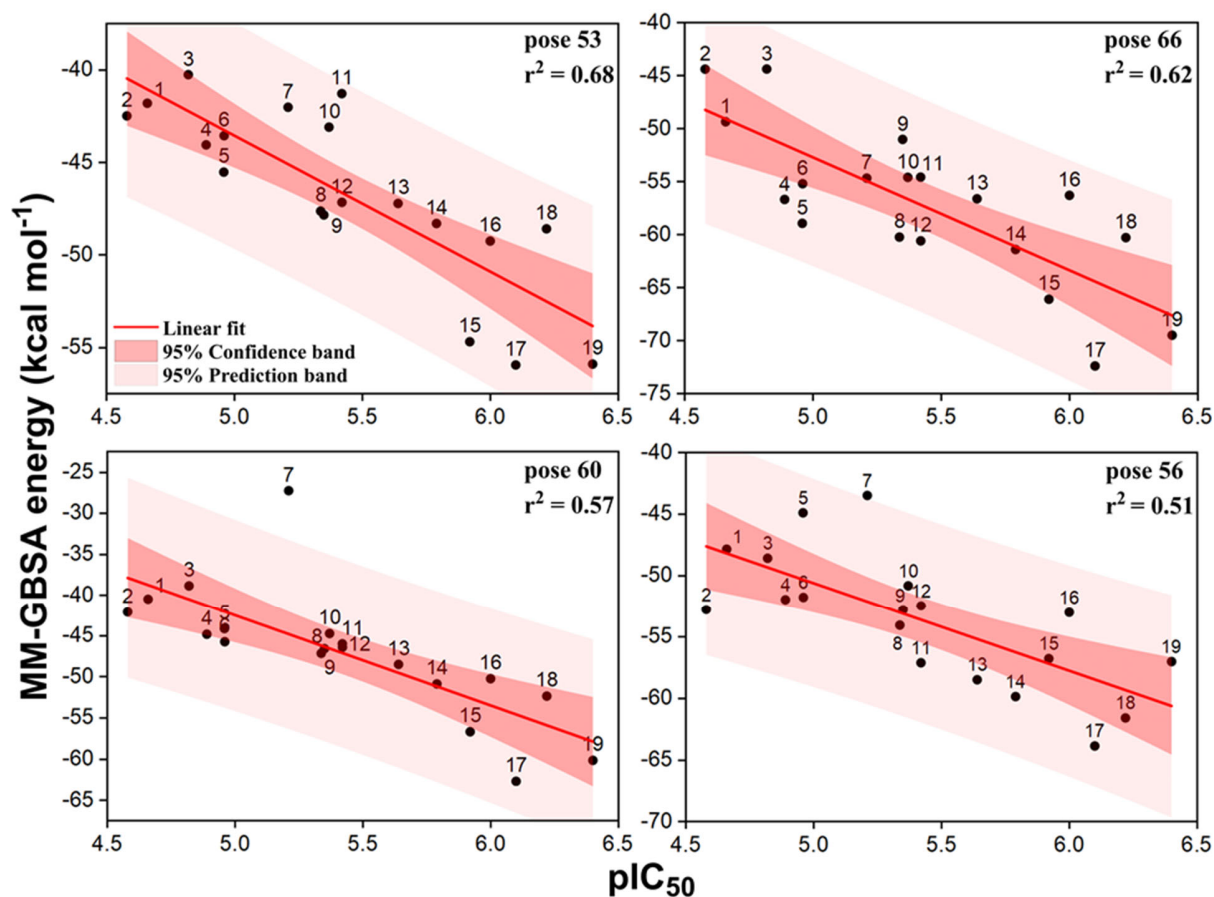


Figure S8. The regression plots between binding energy (y-axis) and pEC₅₀ (x-axis) of PQs 1-19 (Table 1) for the docking poses p53, p56, p60, and p66.

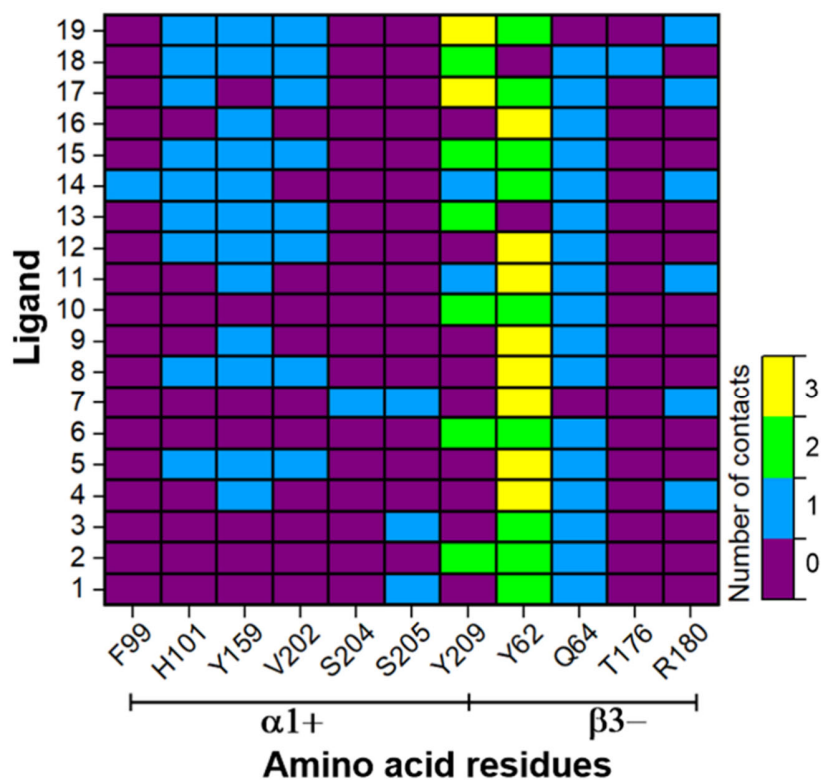


Figure S9. SIFT showing the favorable contacts (hydrogen bond + hydrophobic interactions) for the docking pose 53 (BM I) of PQs 1-19 (Table 1) at the $\alpha 1+$ / $\beta 3-$ interface.

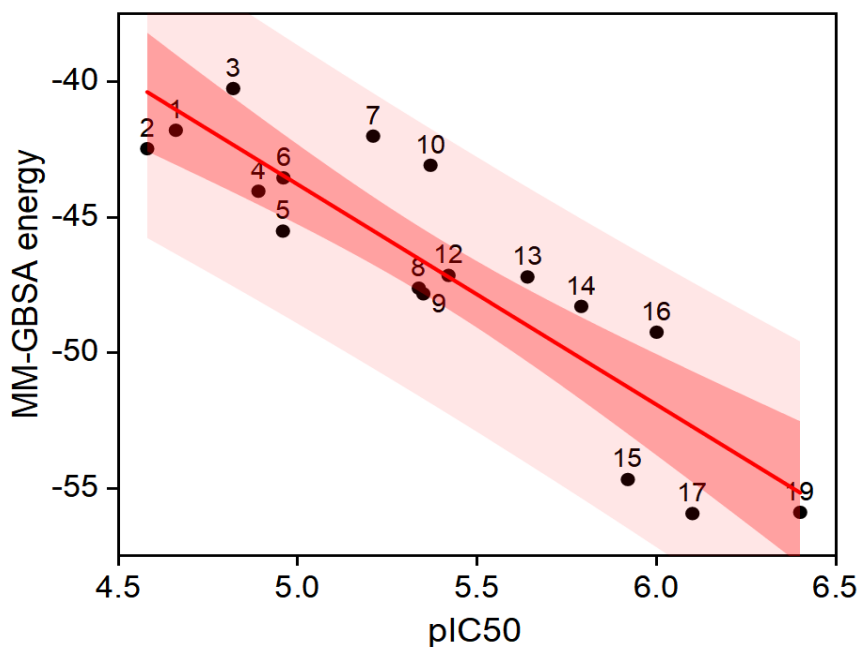


Figure S10. The regression plot between binding energy (y-axis) and pEC₅₀ (x-axis) of PQs after removing outliers (11 and 18) for the docking pose p53; R_{SAR} score = 0.9, r^2 (COD) = 0.79.

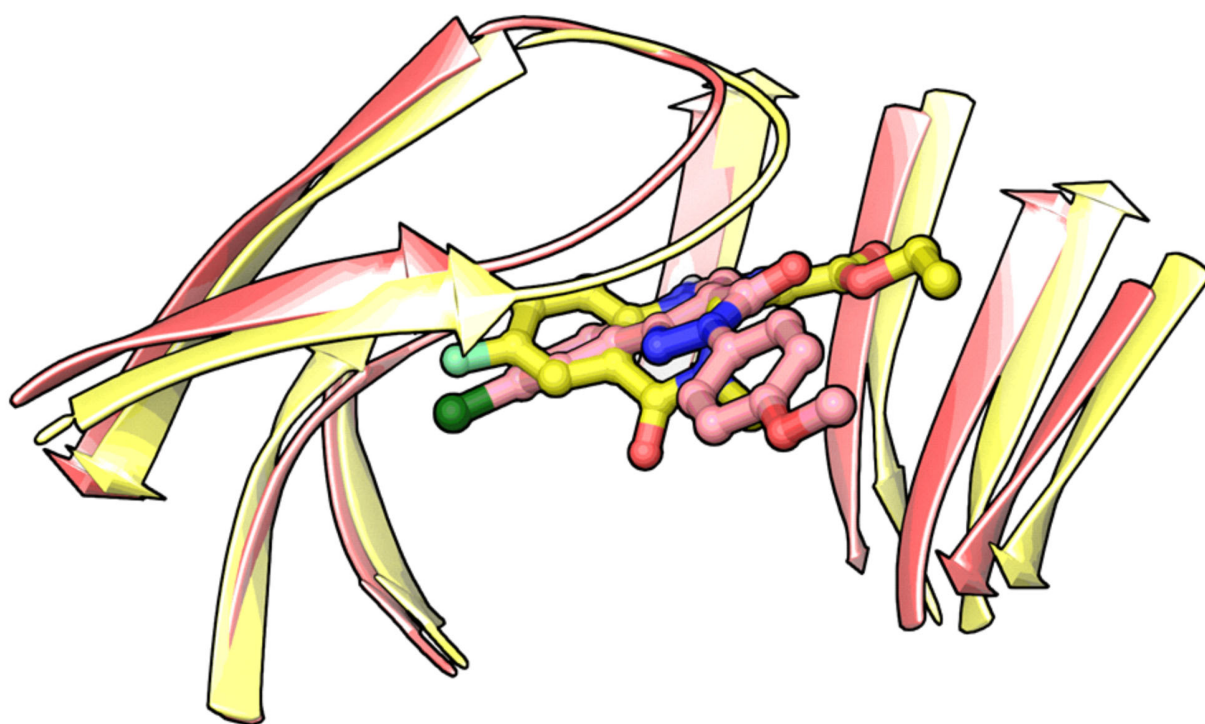


Figure S11. The crystallographic binding mode of flumazenil at the $\alpha1+/\gamma2$ - interface (PDB ID: 6D6U) superposed onto the predicted binding mode of compound **14** (BM I, p53) at the $\alpha1+/\beta3$ - interface. The ligands and subunits are depicted in stick and ribbon style, respectively. The $\alpha1+/\gamma2$ - and $\alpha1+/\beta3$ - interfaces are colored yellow and red, respectively. The carbon atoms of flumazenil and **14** are colored yellow and red, respectively.

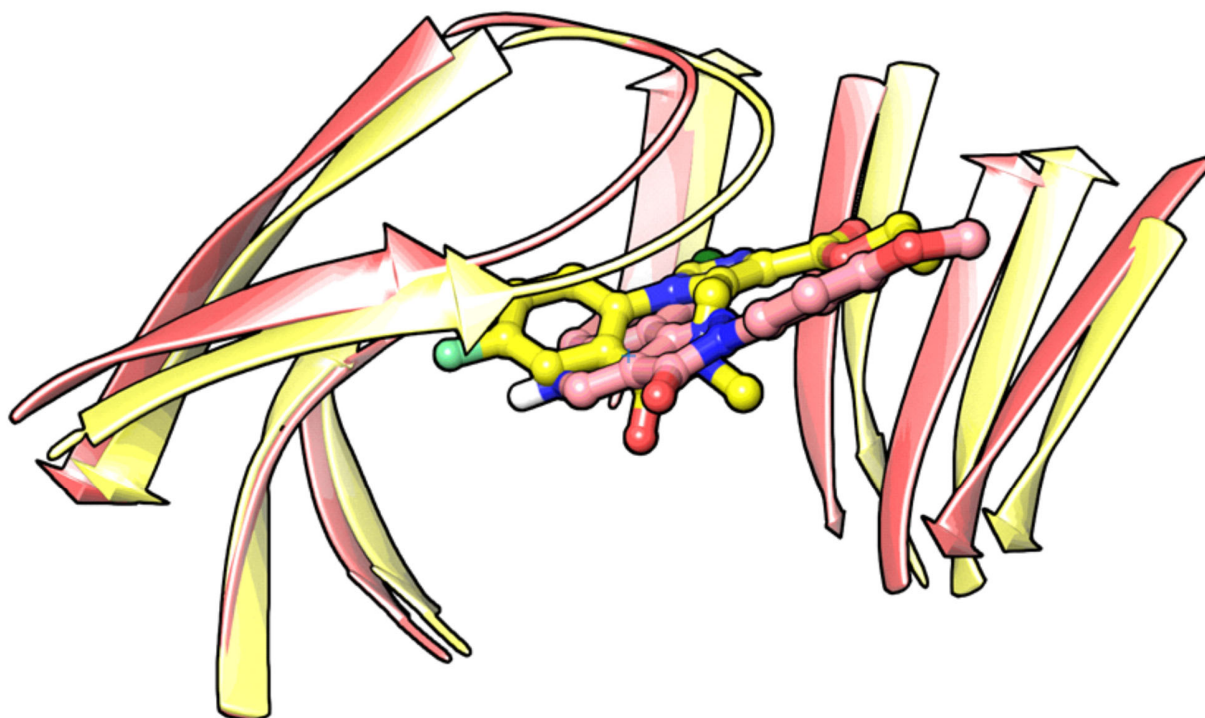


Figure S12. The crystallographic binding mode of flumazenil at the $\alpha 1+/\gamma 2-$ interface (PDB ID: 6D6U) superposed to the predicted binding mode of compound **14** (BM II, p66) at the $\alpha 1+/\beta 3-$ interface. The ligands and subunits are depicted in stick and ribbon style, respectively. The $\alpha 1+/\gamma 2-$ and $\alpha 1+/\beta 3-$ interfaces are colored yellow and red, respectively. The carbon atoms of flumazenil and **14** are colored yellow and red, respectively.

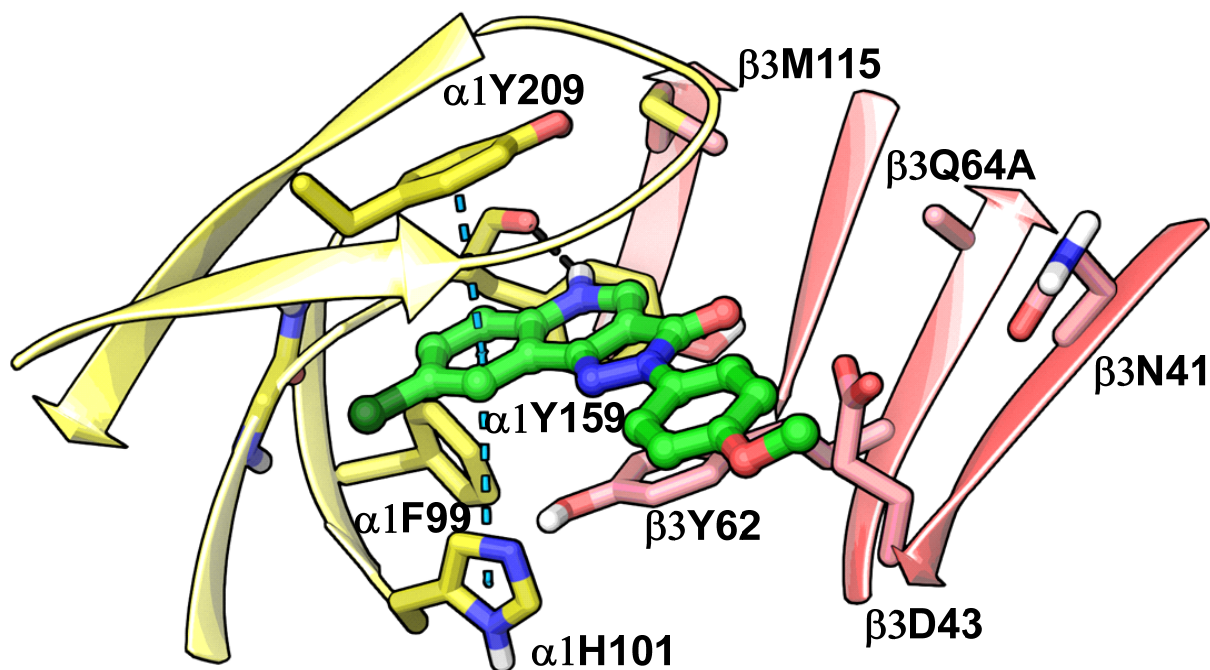


Figure S13. Predicted binding mode of compound 14 (p53, BM I, green) in the $\alpha 1\beta 364A$ mutant; Binding energy: $-57.02 \text{ kcal mol}^{-1}$.

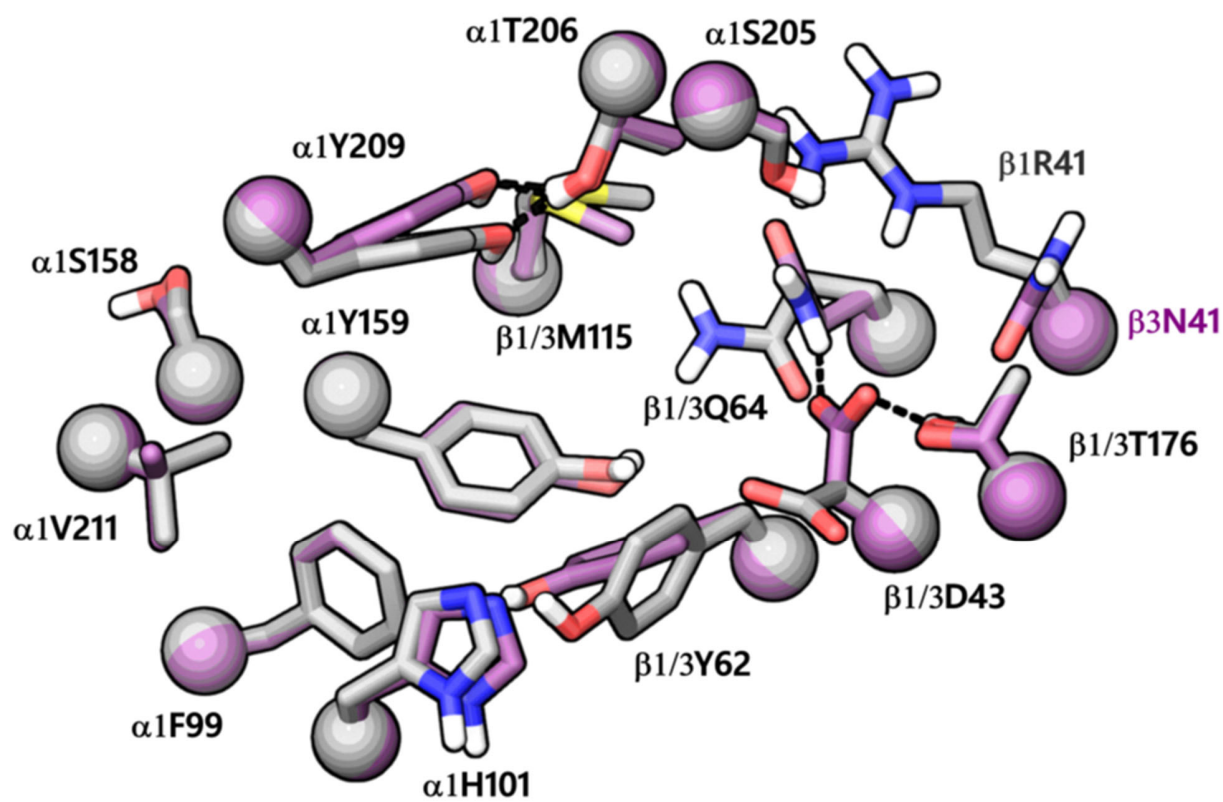


Figure S14. The binding site of the $\alpha 1\beta 3$ subtype superposed to the binding site of the $\alpha 1\beta 1$ subtype. The $C\alpha$ atoms and the side chains of residues are depicted in space-filling and stick style, respectively. The carbon atoms of the residues are colored violet and grey for $\alpha 1\beta 3$ and $\alpha 1\beta 1$. The black dotted lines indicate hydrogen bond interaction.

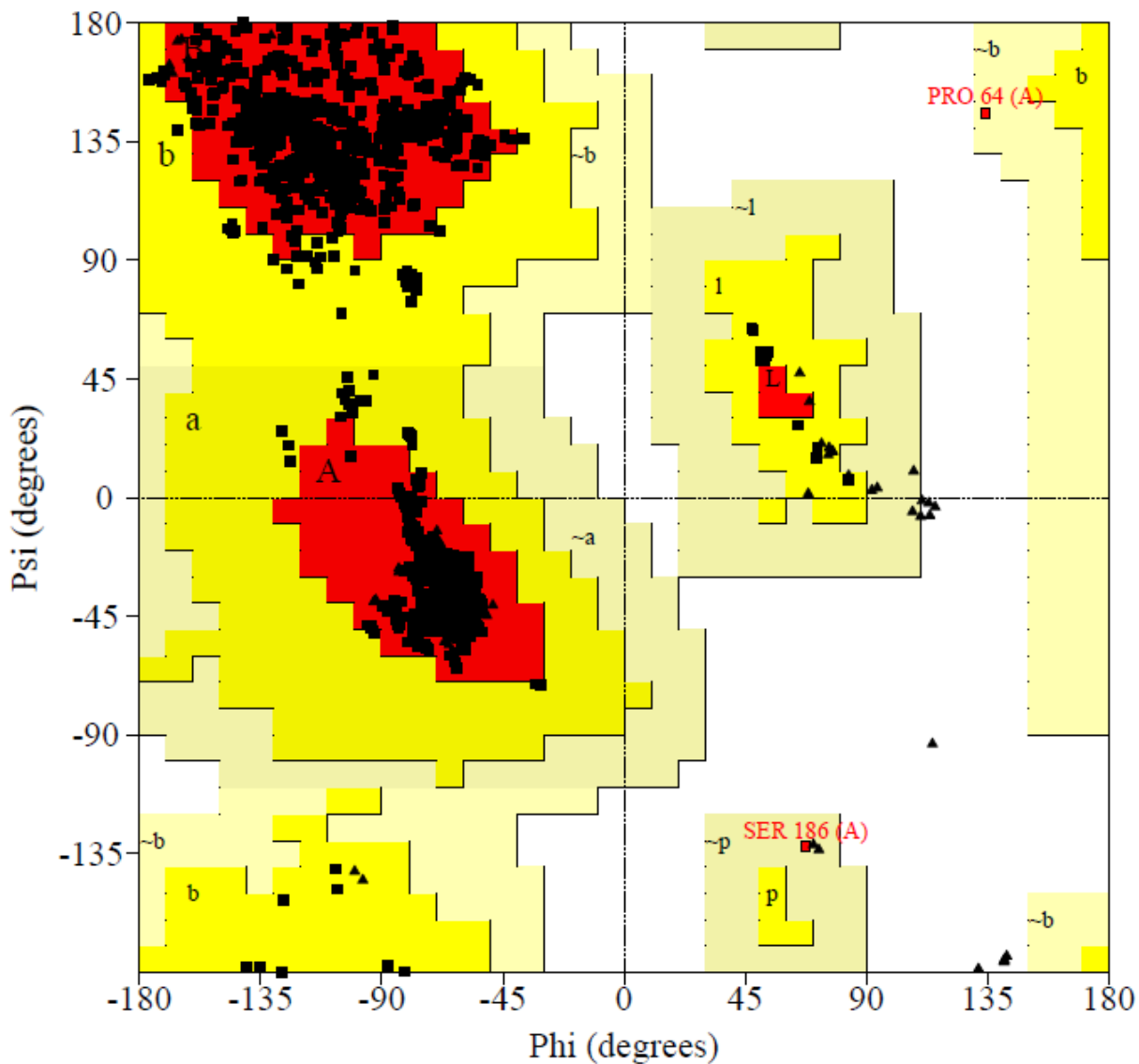


Figure S15. The Ramachandran plot of the $\alpha 1\beta 1\gamma 2$ subtype of the $GABA_A$ receptor based on the 4COF structure.

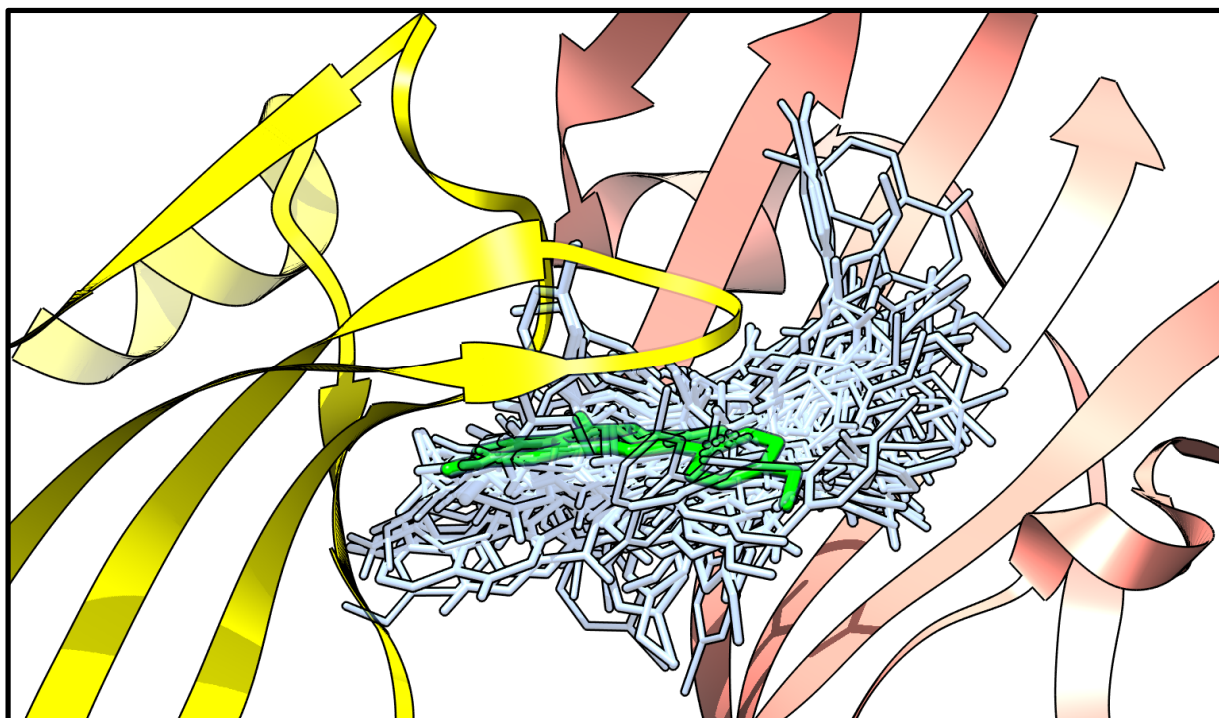


Figure S16. Distribution of the 100 docking poses of PZ-II-028 (**14**) at the $\alpha1+/\beta1-$. Maximum poses are occupying the center of the pocket, while some are partially dislocated outside the pocket. The most favorable pose showing the lowest RMSD to BM I (p53, $\alpha1\beta3$) is indicated in green and is rendered more prominent, while the rest of the poses are depicted in blue and are made less noticeable. The $\alpha1+$ and $\beta1-$ subunits are shown in ribbon style and are colored yellow and red, respectively.